

However, it is located in the moving water phase and could generate an electrokinetic effect.

There are several other experimental facts that could be explained using the zero surface charge DL model.

For instance, Derjaguin, Dukhin, and Yaroschuk applied this model to explain the phenomenon of coagulation zones in the stability of colloids with adsorption layers of nonionic polymers.<sup>5</sup>

Later, Dukhin et al. applied the same ideas for explaining reverse osmosis on uncharged membranes.<sup>6</sup>

Mancui and Ruckenstein applied these ideas for describing surface tension<sup>2</sup> and later to the stability problem.<sup>3</sup>

More recently, Yaroschuk<sup>11</sup> suggested that the shift in the isoelectric point observed by Kosmulski and Rosenholm at high ionic strength<sup>9</sup> is also related to this new DL model.

Alekseyev et al.<sup>12,13</sup> applied similar ideas for explaining their observation of electosmosis at high ionic strength.

It is clearly very important to verify the existence of this zero charge DL and develop methods for studying its structure. This article presents an attempt to achieve this goal. We think that this can be done using nonionic surfactants as a probe to modify the structure of the interfacial layer and thereby shed light on the distribution of charge within this structure.

As described in many publications on this subject, nonionic surfactants have the capacity to shift the position of the slipping plane. We mention here the early work by Glazman in 1966<sup>14</sup> and the most recent paper by the Somasundaran group in 2005.<sup>15</sup> This idea of a nonionic surfactant-induced shift of the slipping plane dominates corresponding chapter of Lyklema's book.<sup>1</sup> In this work, we suggest using the shift in the slipping plane simply as a tool to localize the position of the charge within the interfacial layer.

However, to use the nonionic surfactant as simply a tool to change the structure of the double layer, we must keep in mind that in principle such surfactants might also have an effect on the electrical properties of the double layer. There are two known effects that nonionic surfactants might have on the electric interfacial properties.

First, nonionics reduce the DL capacity by replacing the more polar water molecules with the less polar surfactant molecules, as described in early works by Frumkin and later by Damaskin et al.<sup>16</sup> and mentioned in ref 17. If we assume a constant surface charge, then this replacement should lead to an increased surface potential. We will see that in our experiments the electric potential decreases with nonionic surfactant concentration, so this effect can be ruled out.

Second, the assumption of a constant surface charge might be questionable as well. For instance, Karraker and Radke<sup>17</sup> argued that a nonionic surfactant competes with specifically adsorbed hydroxide ions. This might lead to a substantial reduction of the surface charge. However, their model is valid for the adsorption of charge-determining ions on a fluid surface. In this work, we use solid particles that instead gain surface charge due to a

dissociation mechanism. Therefore, we can most likely rule out this second possibility as well.

Having ruled out the possibilities that the nonionic surfactant might change the electrical properties of the double layer, we can now more confidently attempt to interpret the experimental changes we see as resulting only from changes in the structure (i.e., the position) of the slipping plane.

There is one more factor that must be taken into account, namely, the relationship between nonionic surfactant adsorption and ionic strength. It is known that increasing ionic strength could affect and even completely eliminate the adsorption of nonionic surfactants.<sup>18,19</sup> We should admit that initially we ignored this possibility and only a reviewer's comments forced us to investigate it. To do this, we must have a means for controlling nonionic surfactant adsorption. We will show here that an ultrasound attenuation measurement can serve this purpose.

Ultrasound also offers a means for measuring the  $\zeta$  potential at very high ionic strength, much higher than the traditional electrophoretic technique allows. The best electrophoretic experiments at high ionic strength that are known to us (Martin-Molina et al.<sup>20</sup>) exploit salt concentration up to only 0.5 mol/dm<sup>3</sup> with measurement errors becoming comparable to the measured values around 0.2 mol/dm<sup>3</sup>. The ultrasound-based electroacoustic technique allows us to work at ionic strengths up to 2 mol/dm<sup>3</sup>. It is clearly the better choice for the goal of this article.

In addition, the speed of sound measurement yields information on liquid elasticity and can be used for characterizing water structure. We will show here how this method works for studying the influence of ions on the water structure.

In summary, we electroacoustically measure the  $\zeta$  potential of alumina particles in aqueous KCl solutions at ionic strengths up to 2 mol/dm<sup>3</sup> and with various concentrations of the nonionic surfactant Tween 80. In addition, we monitor surfactant adsorption using an acoustic attenuation measurement. We also show that the addition of KCl enforces water elasticity and consequently its structure.

Unfortunately, collected experimental data will not be sufficient for deriving definite conclusions regarding the zero surface charge DL model. This article should be considered to be an introduction and a summary of the description and testing of methods. We hope that these methods in combination with proper surfactant and electrolyte selection would allow us to gain more detailed information on the interfacial structure at high ionic strength.

## Materials

We used alumina AKP-30 from Sumitomo Chemicals as the dispersed phase. These are well-defined particles with a nominal particle size of 300 nm.

We selected this alumina material for several reasons. First, these particles are quite dense relative to the aqueous media and therefore generate a strong electroacoustic signal. Second, these particles are very strongly charged at low pH and make a stable dispersion even at a moderate ionic strength of 0.01 mol/dm<sup>3</sup>. Third, the  $\zeta$  potential of this alumina dispersion is almost independent of pH in the vicinity of pH 4. Fourth, although these dispersions become unstable at higher ionic strength, the

(11) Yaroschuk, A. E. *J. Colloid Interface Science* **2001**, *238*, 381–384.

(12) Alekseyev, O. L.; Bojko, Y. P.; Ovcharenko, F. D.; Shilov, V. N.; Chubirka, L. A. *Kolloidn. Zh.* **1988**, *50*, 211–216 (English translation available).

(13) Alekseyev, O. L.; Bojko, Y. P.; Pavlova, L. A. *Colloids Surf., A* **2003**, *222*, 27–34.

(14) Glazman, J. M. *Discuss. Faraday Soc.* **1966**, *42*, 255.

(15) Misra, P. K.; Mishra, B. K.; Somasundaran, P. *Colloids Surf., A* **2005**, *252*, 169–174.

(16) Damaskin, B. B.; Petriy, O. A. *Introduction in Electrochemical Kinetics*; Moscow, 1975.

(17) Karraker, K. A.; Radke, C. J. *Adv. Colloid Interface Sci.* **2002**, *96*, 231.

(18) Paria, S.; Khilar, K. C. *Adv. Colloid Interface Sci.* **2004**, *110*, 75–95.

(19) Lyklema, J. *Fundamentals in Colloid and Interface Science*; Academic Press: New York, 1991 Vol. 1.

(20) Martin-Molina, A.; Quesada-Perez, M.; Galisteo-Gonzalez, F.; Hidalgo-Alvarez, R. *Colloids Surf., A* **2003**, *222*, 155–164.

# Electrokinetics at High Ionic Strength and Hypothesis of the Double Layer with Zero Surface Charge<sup>†</sup>

A. Dukhin,\* S. Dukhin, and P. Goetz

Dispersion Technology Inc., 364 Adams Street, Bedford Hills, New York 10507

Received February 23, 2005. In Final Form: June 3, 2005

A growing number of publications in the last two decades have suggested that the structure and other properties of the interfacial water layer can significantly affect the double layer (DL) because of changes in ion solvation energy. Most interesting is the possibility that a double layer might in fact exist, even when there is no electric surface charge at all, solely because of the difference in cation and anion concentrations within this interfacial water layer. Dukhin, Derjaguin, and Yaroschuk suggested this possibility 20 years ago and developed a phenomenological theory. Recently, Mancui and Ruckenstein created more sophisticated microscopic model. In this article, we present our first experimental result regarding the verification of this “zero surface charge” DL model. The electroacoustic technique allows testing at high ionic strength (up to 2 M). As a first step, we confirm the surprising result of Johnson, Scales, and Healy regarding large  $\zeta$  potential of alumina ( $8 \pm 1$  mV) in 1 M KCl. As a second step, we suggest using nonionic surfactant Tween 80 for probing and modifying the structure of the interfacial layer at high ionic strength. The application of surfactant at moderate ionic strength (i.e.,  $<0.1$  mol/dm<sup>3</sup>), as might be expected, reduces the  $\zeta$  potential simply by shifting the slipping plane. However, there is no influence of surfactant on the  $\zeta$  potential observed at high ionic strength. It turns out that a high concentration of KCl simply eliminates surfactant adsorption. We develop a new technique for characterizing the adsorption of nonionic surfactant using an acoustic attenuation measurement. We hope that these methods in combination with a proper surfactant and electrolyte selection would allow us to gain more detailed information on the interface structure at high ionic strength.

## Introduction

For many decades, indeed since the creation of the classical Gouy–Chapman–Stern model,<sup>1</sup> the electric surface charge has been considered to be the main factor in generating a double layer. Lyklema<sup>1</sup> describes in detail many of the sometimes chemically complex ways that charge might appear at the interface. However, if we exclude the more complex situations, the double layer, according to the Gouy–Chapman–Stern (GCS) model, is a simple equilibrium structure resulting from the balance between electrostatic interactions (i.e., between the surface charge and bulk ions) on one hand and the thermal motion of the ions on the other hand. In this sense, the electric surface charge is the cause or the driving force of the DL formation.

However, it long ago became clear that the Gouy–Chapman–Stern theory has a restricted range of validity. Recent papers by Mancui and Ruckenstein<sup>2,3</sup> present a very comprehensive review of various attempts to generalize this theory.

One of the most interesting conclusions of these new DL models is that a separation of electric charge within the interfacial water layer might occur even for uncharged surfaces (i.e., a double layer might exist even without any surface charge). Dukhin, Derjaguin, and Yaroschuk mentioned this possibility for the first time, as far as we know, about 20 years ago.<sup>4–6</sup> These papers are available in English but apparently were unknown to Mancui and Ruckenstein, who repeated this conclusion in their recent papers<sup>2,3</sup> with much better justification.

All of these authors pointed out that the peculiar properties of any surface water layer can affect the solvation energy of ions. Early authors mentioned two potential mechanisms: variation of the dielectric permittivity and image forces.<sup>4</sup> Later authors suggested additional mechanisms such as van der Waals interaction between the ions and media, ion size effects, and changes in the dielectric constant with the magnitude of the electric field.<sup>2</sup>

From a phenomenological viewpoint, all of these mechanisms, and perhaps others as well, lead to the same result, namely, that cations and anions may have quite different abilities to penetrate the surface water layer. This in turn might lead to differences in their concentration within this layer, and, consequently, to a finite electric charge. This finite charge would in turn generate an electric field that then builds a screening diffuse layer in the bulk.

Figure 1 presents two simple cartoons that illustrate the difference between the GCS model and this new “zero surface charge DL” (ZSC). Surface charge in the GCS model is shown as a narrow rectangle that is associated with the solid. The density of the screening charge decays toward the bulk of the solution.

Interfacial charge in the ZSC model is associated with the water phase. Structural peculiarities of the surface water layer diminish toward the bulk. Deviations in ions concentrations induced by this structure would diminish correspondingly. For instance, if the water interfacial structure allows a higher concentration of cations and a

<sup>†</sup> Part of the Bob Rowell Festschrift special issue.

(1) Lyklema, J. *Fundamentals in Colloid and Interface Science*; Academic Press: New York, 1995; Vol. 2.

(2) Mancui, M.; Ruckenstein, E. *Adv. Colloid Interface Sci.* **2003**, *105*, 63–101.

(3) Mancui, M.; Ruckenstein, E. *Adv. Colloid Interface Sci.* **2004**, *112*, 109–128.

(4) Dukhin, S. S.; Yaroschuk, A. E. *Kolloidn. Zh.* **1982**, *44*, 5, 884–895 (English translation available).

(5) Derjaguin, B. V.; Dukhin, S. S.; Yaroschuk, A. E. *J. Colloid Interface Sci.* **1987**, *115*, 234.

(6) Dukhin, S. S.; Churaev, N. V.; Shilov, V. N.; Starov, V. M. *Adv. Chem. USSR* **1988**, *55*, 1010–1029 (English translation: Dukhin, S. S.; Churaev, N. V.; Shilov, V. N.; Starov, V. M. *Adv. Chem. USSR* **1988**, *43*, 6).

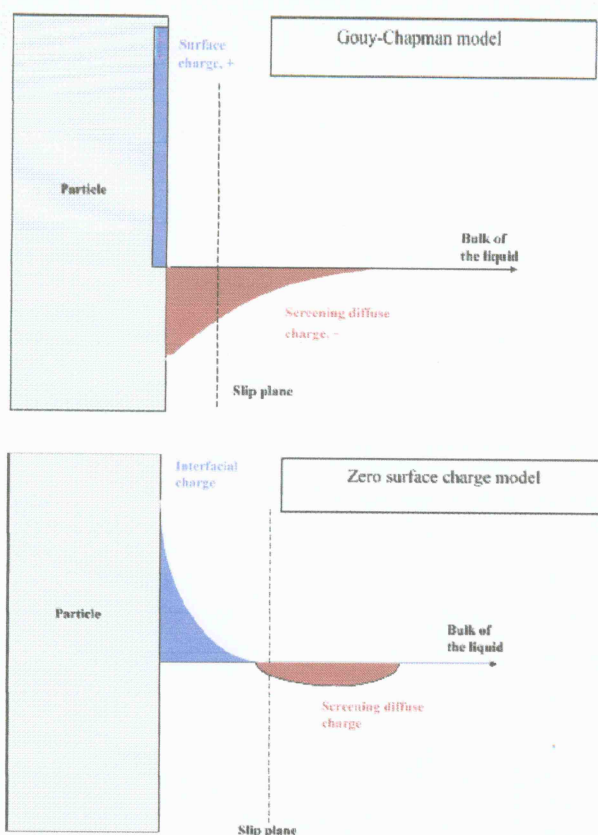


**Figure 1.** Illustration of the GCS and zero surface charge models of the double layer at low and moderate ionic strength. Geometric objects with rectangular and decaying shapes illustrate electric charge densities with opposite signs.

lower concentration of anions, then there would be excessive positive charge within the interfacial layer as shown in Figure 1. The density of this interfacial charge would decline with the structure. This interfacial charge would electrostatically attract counterions (negative in Figure 1). The concentrations of both ion species become equal at some distance from the surface. The charge density becomes zero at this distance as shown in Figure 1. After this point and further away from the surface, the screening charge of counterions begins to build up. Residual peculiarities of the water interfacial structure would still affect the spatial distribution of the screening charge at shorter distances. That is why Figure 1 shows a gradual increase in the screening charge density following decay as in the GCS theory.

This zero surface charge DL can be useful for interpreting several experimental facts. In particular, it explains the existence of the electrokinetic effects at high ionic strength. According to the classic Gouy–Chapman–Stern theory, an increase in the ionic strength must suppress the electrokinetic phenomena due to the collapse of the DL, as shown in Figure 2. However, there are several experimental papers suggesting that electrokinetic phenomena do exist at high ionic strength. The first work known to us was published in 1985 by Deinega et al. and later translated into English.<sup>7</sup> The more recent works are by the Kosmulski and Rosenholm group and are summarized in their recent review.<sup>8</sup>

(7) Deinega, Y. F.; Polyakova, V. M.; Alexandrova, L. N. *Kolloidn. Zh.* **1982**, *48*, 3, 546–548 (English translation available).

(8) Kosmulski, M.; Rosenholm, J. B. *Adv. Colloid Interface Sci.* **2004**, *112*, 93–107.

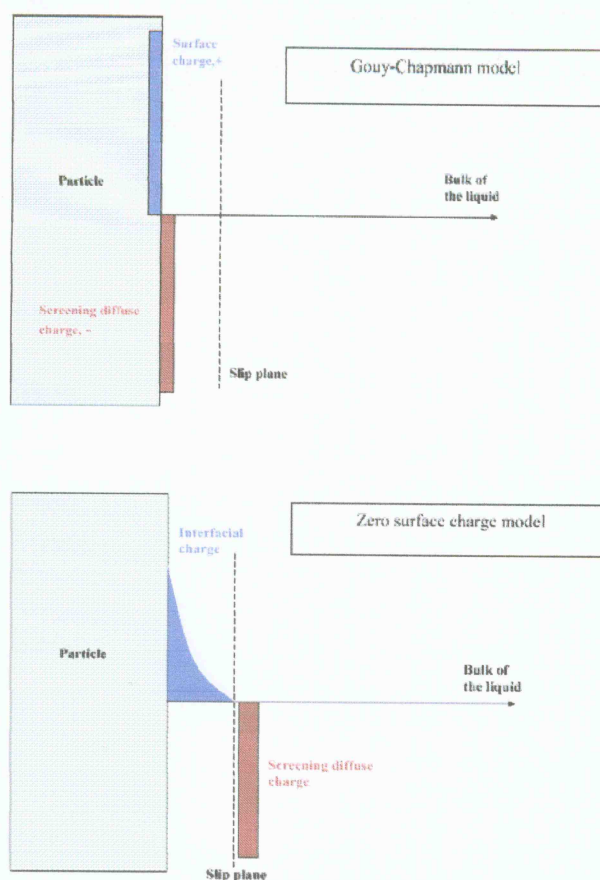


**Figure 2.** Illustration of the GCS and zero surface charge models of the double layer at high ionic strength. Geometric objects with rectangular and decaying shapes illustrate electric charge densities with opposite signs.

There are also papers published by Johnson, Scales, and Healy reporting a  $\zeta$ -potential value on the range of 20–30 mV even at 1 M ionic strength.<sup>9,10</sup> This large value of the  $\zeta$  potential at high ionic strength is very surprising because it cannot be explained within the scope of classical Gouy–Chapman–Stern theory. Modern modifications to this theory, such as corrections for ion sizes, image forces, and other factors listed by Lyklema,<sup>1</sup> make the situation even worse. Figure 3.18 in Lyklema's book shows that all of these factors lead to the reduction of the surface potential for a given surface charge compared to that from GCS classic theory.

This experimental work by Johnson, Scales, and Healy might be an important milestone in studying the interface at high ionic strength. It certainly deserves independent experimental confirmation, ideally with a different instrument. This will be one of the purposes of this article.

These scientists do not offer any theoretical description of the DL structure that leads to a high  $\zeta$ -potential value at high ionic strength. We think that the zero surface charge DL model yields a possible explanation of these experimental facts. Interfacial charge associated with the water structure could extend away from the surface beyond the slipping plane, as shown in Figure 2. The screening charge is collapsed because of high ionic strength.

(9) Johnson, S. B.; Scales, P. J.; Healy, T. W. *Langmuir* **1999**, *15*, 2836–2843.

(10) Johnson, S. B.; Franks, G. V.; Scales, P. J.; Healy, T. W. *Langmuir* **1999**, *15*, 2844–2853.

However, it is located in the moving water phase and could generate an electrokinetic effect.

There are several other experimental facts that could be explained using the zero surface charge DL model.

For instance, Derjaguin, Dukhin, and Yaroschuk applied this model to explain the phenomenon of coagulation zones in the stability of colloids with adsorption layers of nonionic polymers.<sup>5</sup>

Later, Dukhin et al. applied the same ideas for explaining reverse osmosis on uncharged membranes.<sup>6</sup>

Mancui and Ruckenstein applied these ideas for describing surface tension<sup>2</sup> and later to the stability problem.<sup>3</sup>

More recently, Yaroschuk<sup>11</sup> suggested that the shift in the isoelectric point observed by Kosmulski and Rosenholm at high ionic strength<sup>8</sup> is also related to this new DL model.

Alekseyev et al.<sup>12,13</sup> applied similar ideas for explaining their observation of electrosorption at high ionic strength.

It is clearly very important to verify the existence of this zero charge DL and develop methods for studying its structure. This article presents an attempt to achieve this goal. We think that this can be done using nonionic surfactants as a probe to modify the structure of the interfacial layer and thereby shed light on the distribution of charge within this structure.

As described in many publications on this subject, nonionic surfactants have the capacity to shift the position of the slipping plane. We mention here the early work by Glazman in 1966<sup>14</sup> and the most recent paper by the Somasundaran group in 2005.<sup>15</sup> This idea of a nonionic surfactant-induced shift of the slipping plane dominates corresponding chapter of Lyklema's book.<sup>1</sup> In this work, we suggest using the shift in the slipping plane simply as a tool to localize the position of the charge within the interfacial layer.

However, to use the nonionic surfactant as simply a tool to change the structure of the double layer, we must keep in mind that in principle such surfactants might also have an effect on the electrical properties of the double layer. There are two known effects that nonionic surfactants might have on the electric interfacial properties.

First, nonionics reduce the DL capacity by replacing the more polar water molecules with the less polar surfactant molecules, as described in early works by Frumkin and later by Damaskin et al.<sup>16</sup> and mentioned in ref 17. If we assume a constant surface charge, then this replacement should lead to an increased surface potential. We will see that in our experiments the electric potential decreases with nonionic surfactant concentration, so this effect can be ruled out.

Second, the assumption of a constant surface charge might be questionable as well. For instance, Karraker and Radke<sup>17</sup> argued that a nonionic surfactant competes with specifically adsorbed hydroxide ions. This might lead to a substantial reduction of the surface charge. However, their model is valid for the adsorption of charge-determining ions on a fluid surface. In this work, we use solid particles that instead gain surface charge due to a

dissociation mechanism. Therefore, we can most likely rule out this second possibility as well.

Having ruled out the possibilities that the nonionic surfactant might change the electrical properties of the double layer, we can now more confidently attempt to interpret the experimental changes we see as resulting only from changes in the structure (i.e., the position) of the slipping plane.

There is one more factor that must be taken into account, namely, the relationship between nonionic surfactant adsorption and ionic strength. It is known that increasing ionic strength could affect and even completely eliminate the adsorption of nonionic surfactants.<sup>18,19</sup> We should admit that initially we ignored this possibility and only a reviewer's comments forced us to investigate it. To do this, we must have a means for controlling nonionic surfactant adsorption. We will show here that an ultrasound attenuation measurement can serve this purpose.

Ultrasound also offers a means for measuring the  $\zeta$  potential at very high ionic strength, much higher than the traditional electrophoretic technique allows. The best electrophoretic experiments at high ionic strength that are known to us (Martin-Molina et al.<sup>20</sup>) exploit salt concentration up to only 0.5 mol/dm<sup>3</sup> with measurement errors becoming comparable to the measured values around 0.2 mol/dm<sup>3</sup>. The ultrasound-based electroacoustic technique allows us to work at ionic strengths up to 2 mol/dm<sup>3</sup>. It is clearly the better choice for the goal of this article.

In addition, the speed of sound measurement yields information on liquid elasticity and can be used for characterizing water structure. We will show here how this method works for studying the influence of ions on the water structure.

In summary, we electroacoustically measure the  $\zeta$  potential of alumina particles in aqueous KCl solutions at ionic strengths up to 2 mol/dm<sup>3</sup> and with various concentrations of the nonionic surfactant Tween 80. In addition, we monitor surfactant adsorption using an acoustic attenuation measurement. We also show that the addition of KCl enforces water elasticity and consequently its structure.

Unfortunately, collected experimental data will not be sufficient for deriving definite conclusions regarding the zero surface charge DL model. This article should be considered to be an introduction and a summary of the description and testing of methods. We hope that these methods in combination with proper surfactant and electrolyte selection would allow us to gain more detailed information on the interfacial structure at high ionic strength.

## Materials

We used alumina AKP-30 from Sumitomo Chemicals as the dispersed phase. These are well-defined particles with a nominal particle size of 300 nm.

We selected this alumina material for several reasons. First, these particles are quite dense relative to the aqueous media and therefore generate a strong electroacoustic signal. Second, these particles are very strongly charged at low pH and make a stable dispersion even at a moderate ionic strength of 0.01 mol/dm<sup>3</sup>. Third, the  $\zeta$  potential of this alumina dispersion is almost independent of pH in the vicinity of pH 4. Fourth, although these dispersions become unstable at higher ionic strength, the

(11) Yaroschuk, A. E. *J. Colloid Interface Science* **2001**, *238*, 381–384.

(12) Alekseyev, O. L.; Boiko, Y. P.; Ovcharenko, F. D.; Shilov, V. N.; Chubirka, L. A. *Kolloidn. Zh.* **1988**, *50*, 211–216 (English translation available).

(13) Alekseyev, O. L.; Bojko, Y. P.; Pavlova, L. A. *Colloids Surf., A* **2003**, *222*, 27–34.

(14) Glazman, J. M. *Discuss. Faraday Soc.* **1966**, *42*, 255.

(15) Misra, P. K.; Mishra, B. K.; Somasundaran, P. *Colloids Surf., A* **2005**, *252*, 169–174.

(16) Damaskin, B. B.; Petriy, O. A. *Introduction in Electrochemical Kinetics*; Moscow, 1975.

(17) Karraker, K. A.; Radke, C. J. *Adv. Colloid Interface Sci.* **2002**, *96*, 231.

(18) Paria, S.; Khilar, K. C. *Adv. Colloid Interface Sci.* **2004**, *110*, 75–95.

(19) Lyklema, J. *Fundamentals in Colloid and Interface Science*; Academic Press: New York, 1991 Vol. 1.

(20) Martin-Molina, A.; Quesada-Perez, M.; Galisteo-Gonzalez, F.; Hidalgo-Alvarez, R. *Colloids Surf., A* **2003**, *222*, 155–164.

soft deposit formed on settling can easily be redispersed with sonication. This property of alumina suspension becomes very useful for electroacoustic measurements. It allows the measurement of supernatant liquid separately from particles without a complicated centrifugation procedure.

In addition, these alumina particles were used in the work by Johnson, Scales, and Healy,<sup>9,10</sup> which we are going to confirm.

We used potassium chloride (J. T. Baker Chemical Co.) as means for varying the ionic strength of the aqueous dispersions.

We use nonionic surfactant polysorbate 80 (aka Tween 80, Spectrum Chemical), as is, with no purification. This liquid is quite viscous and requires some effort to dissolve properly in water. That is why we prepare a 5:1 diluted aqueous solution of this surfactant for use in automated titration procedures. This dilution requires a long period of mixing of the surfactant-water solution with a magnetic stirrer.

### Measurement Technique

There are two different characterization techniques based on ultrasound: acoustics and electroacoustics. We measured all parameters using the Dispersion Technology DT-1200, which has both sensors. Here we give a short description of both.

**Acoustics.** The acoustic sensor of DT-1200 is built as a "transmission" technique. A piezoelectric transducer converts an input electrical tone burst to an ultrasound pulse of a certain frequency ( $f$ ) and intensity ( $I_{in}$ ) and launches it into the sample. The intensity of this pulse decays as it passes through the sample because of the interaction with the fluid. A second piezoelectric transducer converts this weakened acoustic pulse back to an electric pulse and sends it to the electronics for comparison with the initial input pulse. The output pulse intensity ( $I_{out}$ ) and time delay ( $t$ ) from the input to output transducer for each frequency and gap ( $L$ ) can be considered to be the raw data from which further interpretation is made. It is convenient to present these raw data in terms of attenuation coefficient  $\alpha$  and speed of sound  $V$  using the following equations:

$$\alpha[\text{dB/cm MHz}] = \frac{1}{f[\text{MHz}] L[\text{cm}]} \log \frac{I_{in}}{I_{out}} \quad (1)$$

$$V[\text{m/s}] = \frac{L[\text{m}]}{t[\text{s}]} \quad (2)$$

Attenuation frequency spectra and the speed of sound are normal experimental output of the acoustic spectrometer.

These experimental data could be used either for empirical correlation with other properties of the system under investigation or for further theoretical treatment. In this article, we will correlate these measured parameters with the concentrations of surfactant and KCl.

We also use acoustic attenuation spectra for characterizing the particle size distribution using the theoretical procedure presented in ref 21.

**Electroacoustic Measurements.** Debye<sup>22</sup> first predicted an electroacoustic effect 70 years ago. In either electrolyte solutions or dispersions, the effect is related to a coupling between electrodynamic and mechanical phenomena. For instance, the transmission of ultrasound through an electrolyte solution or dispersion generates a current, which is usually referred to as an ion/colloid vibration current. The instrument that we use, DT-1200, has a probe for measuring this electroacoustic signal. This probe can either be installed directly into the DT-1200 sample chamber or optionally in an external sample container, as shown in Figure 3. This flexibility is a very convenient feature of this instrument because it allows a complete measurement of both the particle size and  $\zeta$  potential of the dispersed sample in the DT-1200 sample chamber or the measurement of just the supernatant of the settled sample in an external vessel.

The electroacoustic measurement of the  $\zeta$  potential involves three steps.<sup>21</sup>

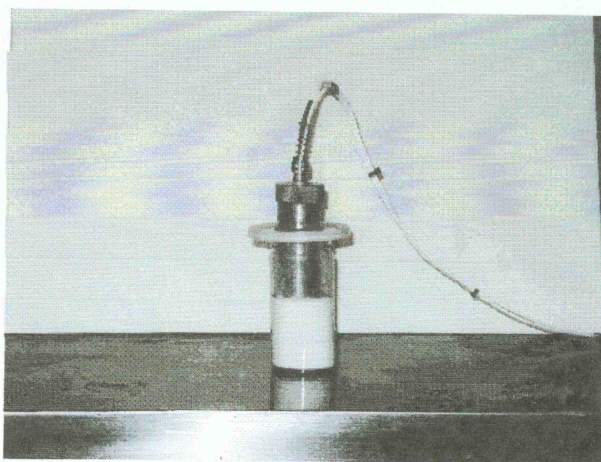


Figure 3. Photograph of the DT-300 zeta potential probe inserted into the alumina dispersion.

The first step is calibration with 10% silica Ludox in a 0.01 M KCl aqueous solution. The  $\zeta$  potential of this dispersion is  $-38$  mV, which is the basis for calibration. We use the same system for verifying results and confirming the performance of the CVI probe. To do this, we measure this system after all titrations or long experiments. The stability of  $\zeta$ -potential reading would confirm that the probe has functioned properly during the experiment.

The second step is the measurement of the electroacoustic signal of the supernatant. This gives us the value of the background signal, the so-called ion vibration current (IVI). This signal must be subtracted later from the electroacoustic signal measured for dispersion. The DT-1200 software allows us to save this value and subsequently to subtract this background signal from further measurements. It is a vector subtraction because the electroacoustic signal is a vector with a certain magnitude and phase. As a simple test that this subtraction works, we measured the supernatant again, this time using the background subtraction. This test gives us the value of the noise level of the electroacoustic measurement. This noise level was orders of magnitude less than the measured signal for all tested dispersions.

This background subtraction allows us to extract the contribution of just the particles, which is then the source for calculating the  $\zeta$  potential. This background subtraction procedure becomes important when the contribution of ions becomes comparable to the contribution of particles. For our alumina dispersions, this subtraction becomes important at an ionic strength above 0.1 mol/dm<sup>3</sup>. The presence of surfactant does not affect this background signal.

The third step is the actual measurement of the electroacoustic signal generated by alumina dispersions.

The calculation of the  $\zeta$  potential from the measured CVI requires information about the particle size distribution. It is an important correction in this case because the particle size distribution varies substantially with ionic strength because of aggregation. The acoustic sensor of the DT-1200 allows us to characterize the particle size without dilution.<sup>21</sup> All of the details of these measurements are given in Appendix 2.

The calculation of the  $\zeta$  potential from the measured CVI also requires an appropriate theory. For this purpose, we can use a "thin" DL approximation<sup>23</sup> because the particle radius  $a$  is much larger than the Debye length  $\kappa^{-1}$  for all of the dispersions used here. The minimum value of the parameter  $\kappa a$  in these experiments is 51 for 0.01 mol/dm<sup>3</sup> KCl. A large  $\kappa a$  value dramatically reduces the influence of the surface conductivity. It turns out that this effect must be taken into account only for the system with 0.01 M KCl. In this case,  $Du = 0.032$ , which causes about a 10% correction in the  $\zeta$ -potential value. The reader can find the definition of the Dukhin number  $Du$  in the ref 24 and a detailed account of the electroacoustic thin DL theory in our book.<sup>21</sup>

(21) Dukhin, A. S.; Goetz, P. J. *Ultrasound for Characterizing Colloids*; Elsevier: Amsterdam, 2002.

(22) Debye, P. J. *Chem. Phys.* **1933**, *1*, 13-16.

(23) Dukhin, A. S.; Shilov, V. N.; Ohshima, H.; Goetz, P. J. *Langmuir* **1999**, *15*, 20, 6692-6706.

The average measurement time for these samples is about 6 min. These systems require continuous mixing to prevent settling, and this mixing is provided by a built-in magnetic stir bar in the DT-1200 sample chamber.

### Experimental Protocols

We used four different experimental protocols. There are multiple measurements for several different dispersions involved in each protocol. There are several preparations of the same chemical compositions for testing reproducibility. Altogether, there were 291 measurements made.

**Ionic Strength Dependence Protocol.** The purpose of this experimental protocol is to determine the  $\zeta$ -potential dependence on ionic strength. We use an alumina dispersion at 3 vol %. There is no dilution involved. The initial dispersion is prepared with 0.01 M KCl solution with the pH adjusted to 4. Sonication for 2 min disperses the particles. Then, additional KCl powder adjusts the ionic strength to the desired value. This increase in ionic strength makes the dispersion unstable and the particles settle. After sedimentation creates a layer of clear supernatant, we insert the zeta probe into this layer. This allows us to measure the background ionic current. It is saved as a calibration constant. The next step is the measurement of the dispersion. After 2 min of sonication, which again mixes the supernatant with the particles, we place the dispersion into the DT1200 measurement chamber. After the measurement with this dispersion is finished, we go to the next one. The measured sample is saved for a repeat measurement some time later.

**Dilution Protocol.** The purpose of this test is to confirm that the measured electroacoustic signal indeed comes from the particles. It is supposed to be a monotonically increasing function of the dispersed-phase volume fraction. This function is practically linear at low and moderate volume fractions under 10%. To test this dependence, we prepared 0.5 L of a 3 vol % dispersion at an ionic strength of 1 mol/dm<sup>3</sup>. This dispersion was unstable, and the particles settled quickly. We removed the clear-layer supernatant and saved it for further dilutions. The deposit is very soft, and we can easily redisperse it with sonication. The weight of this deposit was sufficient for recalculating the volume fraction of particles in the resulting dispersion. It turns out to be 10.7 vol %. We measure this dispersion and then use the supernatant for preparing consequent dilutions at volume fraction of 7, 5, and 3%. The results of these measurements are presented below. This test clearly confirms that the measured electroacoustic signal after background subtraction comes from particles.

**Surfactant Titration Protocol.** The purpose of this experiment is the modification of the interfacial layer. We use a nonionic surfactant for modifying just the structural properties of this layer, maintaining the same surface charge. Nonionic surfactant is supposed to shift the slipping plane and, consequently, reduce the  $\zeta$  potential. We could use the automatic titration option of the DT-1200 for this purpose. We place 5-fold-diluted Tween 80 into a reagent bottle. The titration protocol is specified as 20 consecutive measurements with a total injected volume of 20 mL. The equilibration time after each injection is 30 s. Each measurement employs all probes of the DT-1200. We ran these titrations for four different systems with ionic strengths of 0.01, 0.1, 1, and 2 M KCl.

**Surfactant Adsorption Measurement.** The purpose of this experiment is to develop a procedure for characterizing the concentration of surfactant in the liquid and, consequently, its adsorption. We used a solution of nonionic surfactant with different concentrations to create the calibration curve. Appendix 1 presents the details of this procedure and the corresponding results. We used this calibration curve for determining the concentration of surfactant in supernatant solutions of various alumina dispersions. It is possible to collect the supernatant of a 3 vol % alumina dispersion that is just due to sedimentation. The supernatant of the more concentrated alumina dispersion at 12.3 vol % requires centrifugation.

(24) IUPAC Instruction, *Measurement and Interpretation of Electrokinetic Phenomena*; Physical and Biophysical Division, Project 2001-035-1-100, www.iupac.org.

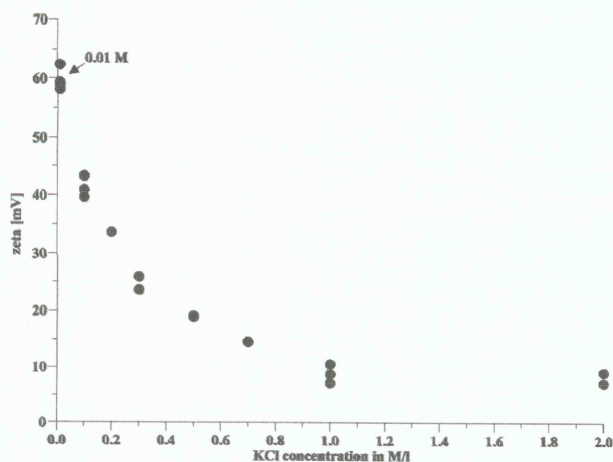


**Figure 4.**  $\zeta$  potential of alumina AKP30 at 3 vol % vs KCl concentration.

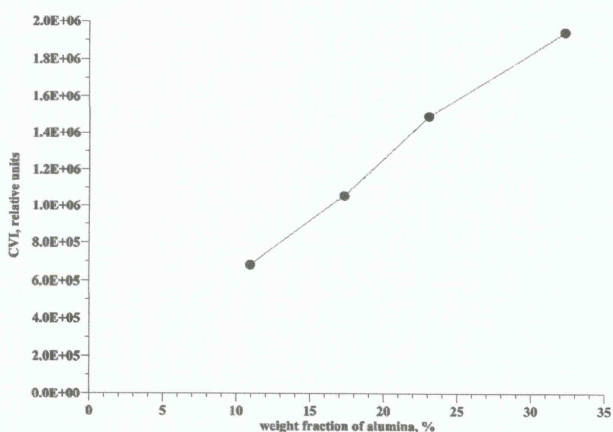


**Figure 5.** Colloid vibrational current of alumina AKP30 in 1 mol/dm<sup>3</sup> KCl solutions at different volume fractions of alumina.

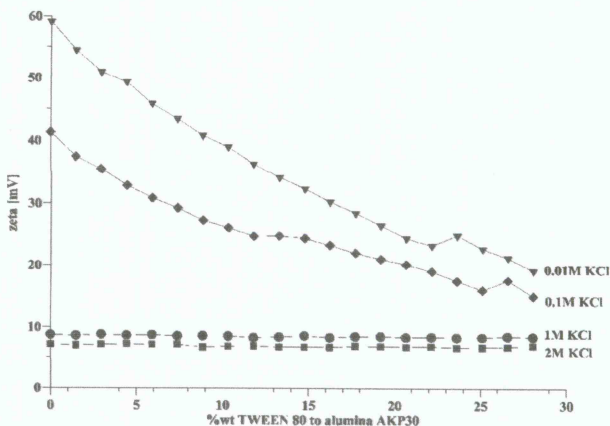


**Figure 6.** Dependence of the alumina AKP30 (3 vol %)  $\zeta$  potential from the concentration of Tween 80 at different KCl concentrations.

### Results and Discussion

The results of these experiment protocols are summarized in Figures 4–7.

Figure 4 shows the dependence of the  $\zeta$  potential on ionic strength as determined using the first experimental protocol. Multiple points at the same KCl concentration correspond to measurements of individually prepared samples. Such repeat measurements provide a rigorous

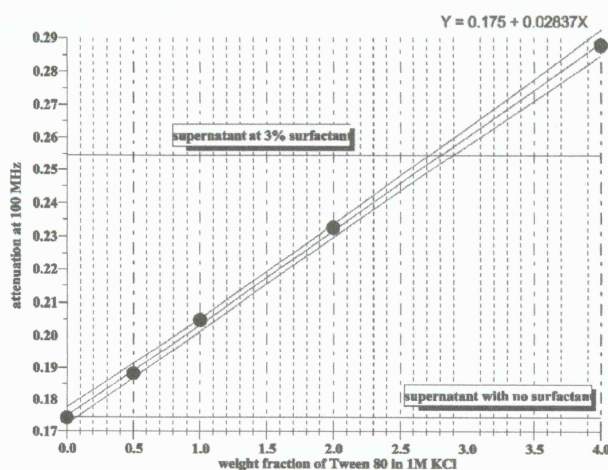


**Figure 7.** Attenuation at 100 MHz vs the concentration of Tween 80 in a 1 M KCl solution. Horizontal lines mark the measured attenuation of the alumina dispersions' supernatant.

reproducibility test with regard to both the phenomena and the instrument performance.

The decay of the  $\zeta$  potential with increasing ionic strength is well documented and predicted by classical GCS DL theory. However, GCS theory tells us that the  $\zeta$  potential should asymptotically approach zero. All generalizations of the GCS theory described in the Lyklema book,<sup>1</sup> by taking into account ion size, image, forces, and so forth, would make this prediction even stronger. Our experiment indicates that GDS theory is not correct with this prediction for these alumina dispersions. At this point, we can only conclude that there is a DL component that does not go to 0 at high ionic strength.

We performed a special dilution test for confirming that the observed electroacoustic signal indeed comes from the particles and is not an artifact. Figure 5 shows that the measured CVI signal is practically a linear function of the alumina particles' weight fraction. This is definite proof that it is generated by particles and related to the properties of the particles.

This result agrees with previous measurements by Johnson, Scales, and Healy for the same dispersion at least on a qualitative level. Both experiments indicate the existence of a  $\zeta$  potential in the range of tens of millivolts in the alumina dispersion at 1 M KCl. There is a discrepancy in the absolute numbers:  $8 \pm 1$  mV in this work compared to about 25 mV in ref 9. We think that this difference could be related to the difference in calibration procedures. The instrument employed in ref 9 (AcoustoSizer) applies an electric field as the driving force, whereas DT-1200 from this article uses ultrasound as the driving force. The AcoustoSizer requires a special calibration procedure to deal with high ionic strength, according to ref 9. The DT-1200 does not need it; it can function properly with the same calibration within the full conductivity range. There are also some comments on complications with the calculation of the  $\zeta$  potential from the measured electroacoustic signal in ref 9. This might also contribute to the differences between our results.

However, the following general conclusion remains: an alumina dispersion exhibits a surprisingly large  $\zeta$  potential at high ionic strength.

In the last experiment, we use nonionic surfactants to modify the structural properties of the interfacial layer. The advantage of using nonionic surfactants is that they supposedly do not affect the surface charge. At the same

**Table 1.** Acoustic Properties of Distilled Water and 1 M KCl Solutions with Various Concentrations of Tween 80

chemical name	speed of sound [m/s] at 25 C°	attenuation at 100 MHz [dB/cm/MHz]
distilled water	1496	0.2034 $\pm$ 0.001
0% surfactant in 1 M KCl	1541.9 $\pm$ 0.36	0.1742 $\pm$ 0.0013
0.5% surfactant in 1 M KCl	1545.4 $\pm$ 0.5	0.1881 $\pm$ 0.0013
1% surfactant in 1 M KCl	1545.6 $\pm$ 0.37	0.2048 $\pm$ 0.0012
2% surfactant in 1 M KCl	1547.21 $\pm$ 0.46	0.2326 $\pm$ 0.0006
3% surfactant in 1 M KCl	1548.4 $\pm$ 0.43	0.2608 $\pm$ 0.005
4% surfactant in 1 M KCl	1550.85 $\pm$ 0.34	0.2877 $\pm$ 0.0025

time, they shift the position of the slipping plane, which should cause a decrease of the  $\zeta$  potential.

Figure 6 shows how the  $\zeta$  potential of the alumina particles changes with increasing concentration of Tween 80 at different ionic strength. Titration curves at 0.01 and 0.1 M agree well with the previous experiments and theory. This confirms that Tween 80 indeed shifts the position of the slipping plane. We can even calculate the distance of this shift ( $d$ ) following procedure described by Hunter.<sup>25</sup> There is a simple relationship between the  $\zeta$  potential with surfactant of a certain concentration ( $\zeta_c$ ) and the  $\zeta$  potential without surfactant ( $\zeta_0$ )

$$\frac{\tanh\left(\frac{\zeta_0}{4}\right)}{\tanh\left(\frac{\zeta_c}{4}\right)} = \exp(\kappa d) \quad (3)$$

where  $\zeta = F\zeta/RT$ ,  $F$  is the Faraday constant,  $R$  is the gas constant, and  $T$  is the absolute temperature.

We can apply this equation to the system with 0.01 M KCl with a Debye length at this concentration of about 3 nm. This leads us to the conclusion that the shift of the slipping plane at this ionic strength achieved by 30% Tween 80 is about 3 nm.

Surprisingly, there is practically no effect of the surfactant on the  $\zeta$  potential at high ionic strength. Titration curves at high ionic strengths of 1 and 2 M show practically no influence of the surfactant (Figure 6).

Initially, we interpreted this result as confirmation that DL has a completely different nature at high ionic strength. However, a reviewer of this paper pointed out that there might be a much simpler explanation, suggesting that the high concentration of KCl could simply eradicate surfactant adsorption. This comment forced us to make an additional test for studying adsorption at high ionic strength.

We have developed a procedure using ultrasound attenuation for measuring the concentration of nonionic surfactant in liquids, including supernatants. Appendix 1 describes this procedure.

It turns out that reviewer of this paper was correct. Figure 7 shows that the attenuation of the supernatant that comes from alumina prepared with 3% surfactant corresponds to the 1 M KCl solution with almost 3% surfactant. This means that particles adsorb practically no surfactant. Tables 1 and 2 give numbers for these two liquids.

To get additional confirmation, we repeated this test with a much higher concentration of alumina: 12.3 vol %. There is still no difference between the attenuation of this dispersion supernatant and the calibration solution with 3% surfactant, as shown in Table 2.

(25) Hunter, R. J. *Zeta Potential in Colloid Science*; Academic Press: London, 1981.

**Table 2. Acoustic Properties of Supernatant Solutions Coming from Alumina AKP 30 Dispersions in 1 M KCl Solutions with Different Surfactant Content<sup>a</sup>**

chemical name	speed of sound [m/s] at 25 C°	attenuation at 100 MHz [dB/cm/MHz]
3 vol % alumina with 25 wt % surfactant relative to alumina	1544.3 ± 0.34	0.2546 ± 0.0008
3 vol % alumina with no surfactant	1541.5 ± 0.29	0.1745 ± 0.001
12.3 vol % alumina with 3% surfactant relative to liquid	1548.7 ± 0.23	0.2597 ± 0.004

<sup>a</sup> Alumina content is shown relative to the dispersion.

We can conclude that KCl at high concentration prevents the adsorption of nonionic surfactant Tween 80 on the surface of alumina particles. This underlines the importance of the proper selection of the surfactant and electrolyte for achieving goals that are formulated. Unfortunately, the nonionic surfactant that we use in this work does not serve this purpose because it loses its adsorption ability at high ionic strength. Following standard terminology (see Lyklema,<sup>19</sup> eq 5.4.11), it is "salted-in" by KCl that apparently increases the solubility of Tween 80. This is a more exceptional situation. Usually, an electrolyte "salts-out" a nonionic surfactant by decreasing its solubility. This justifies our hope of finding another nonionic surfactant that would retain its ability to adsorb at high ionic strength. Procedures that we develop in this work would help us to make this choice.

### Conclusions

We have established that alumina exhibits a significant  $\zeta$  potential ( $8 \text{ mV} \pm 1 \text{ mV}$ ) at very high ionic strength up to  $2 \text{ mol/dm}^3$  of KCl. This is qualitative confirmation of the results published previously by Johnson, Scales, and Healy.<sup>9</sup> Nonionic surfactant (Tween 80) reduces the  $\zeta$  potential by shifting a slip plane in the range of moderate ionic strength ( $< 0.1 \text{ mol/dm}^3$ ). There is no influence of the surfactant on the  $\zeta$  potential observed at high ionic strength. We develop a special method for measuring the adsorption of nonionic surfactant using ultrasound attenuation. This method indicates that this nonionic surfactant does not adsorb at a high concentration of KCl. This explains why it does not affect the  $\zeta$  potential at high ionic strength. The combination of methods that have been developed in this work could be used for the further investigation of the DL structure at high ionic strength.

### Appendix 1. Characterization of Adsorption Using Acoustics.

It is known that acoustic properties of liquids (speed of sound and attenuation) are sensitive to the chemical composition of the liquids including dissolved species.<sup>21</sup> This fact can be used for monitoring the concentration of various chemicals in the supernatant and, consequently, for characterizing the adsorption of these chemicals. We use this method for characterizing the adsorption of Tween 80 by alumina particles.

Table 1 presents the acoustic properties of 1 M KCl solutions with different concentrations of Tween 80. We collected these data using the acoustic sensor of the DT-1200. There is no temperature control. Speed of sound values are corrected for temperature variation assuming  $2.4 \text{ m s}^{-1} \text{ }^\circ\text{C}^{-1}$ . Each system has been measured at least seven times, which allowed us to determine the average absolute variation given in Table 1.

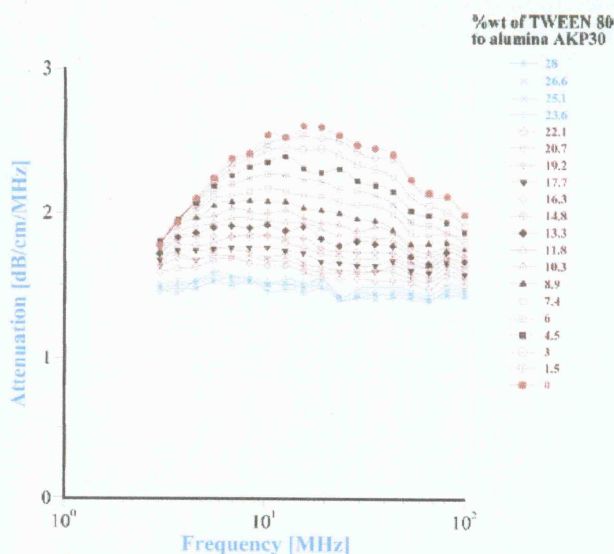


**Figure 8.** Attenuation curves for the alumina dispersion with different concentrations of Tween 80 for a  $0.01 \text{ mol/dm}^3$  KCl solution.

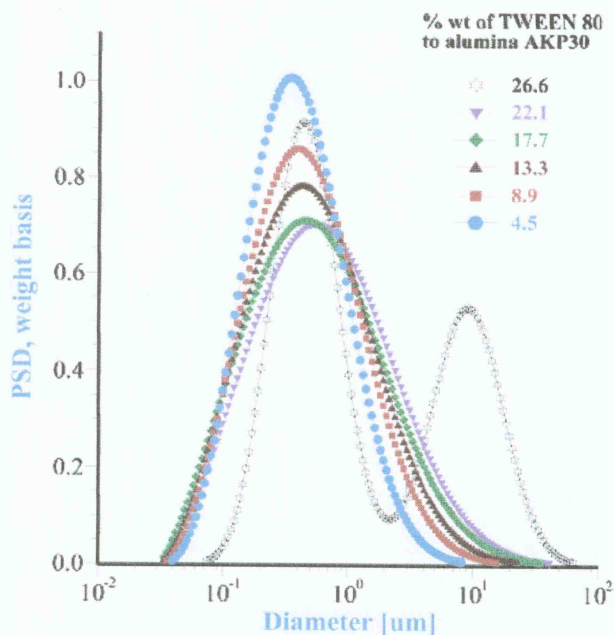


**Figure 9.** Particle size distribution of the alumina with different concentrations of Tween 80 for a  $0.01 \text{ mol/dm}^3$  KCl solution.

It is clearly seen that these parameters are dependent on both the concentration of KCl and the concentration of surfactant. At the same time, these chemicals affect the speed of sound and attenuation differently.

**Speed of Sound.** Inorganic ions of 1 M KCl solution increase the speed of sound by 45 m/s, as one can see by comparing results for distilled water and 1 M KCl in Table 1. The influence of 4% Tween 80 is more than 5 times less, only about 8 m/s.

**Attenuation.** Surfactant at 4% affects the attenuation much more than 1 M KCl; see Table 1. It changes the attenuation by about  $0.11 \text{ dB/cm MHz}$ , whereas 1 M KCl generates only a  $0.03 \text{ dB/cm MHz}$  decrease.

This simple analysis indicates that the speed of sound is a much better parameter for monitoring the concentra-

tion of KCl, whereas attenuation at 100 MHz is a much better parameter for monitoring the concentration of Tween 80.

At the same time, attenuation is not very sensitive to the temperature variation. This also makes it more attractive for characterizing adsorption.

We plot the attenuation data for these surfactant solutions in Figure 7. This practically linear dependence can be used for estimating the concentration of Tween 80 to a precision of a few tenths of a percent.

### Appendix 2. Particle Size Characterization

It is well known that acoustic spectroscopy is valid technique for characterizing the particle size distribution in concentrates. The reader can find more details on this subject in our book.<sup>21</sup> This method is especially suitable for this work because it is independent of the electric properties. In this Appendix, we just give a short overview of this particle-sizing technique as it relates to these alumina dispersions.

The attenuation frequency spectrum is the raw data from which the particle size distribution is calculated. Figure 8 shows these attenuation curves for the alumina dispersion having the lowest ionic strength ( $0.01 \text{ M/dm}^3$ ) with different concentrations of Tween 80. The gradual evolution of the attenuation spectra reflects the variation of the particle size distribution with added surfactant.

The procedure and theory for the calculation of the particle size distribution from these attenuation spectra are given in our book.<sup>21</sup> Figure 9 simply presents the results of these calculated particle size distributions. Note that the particle size monotonically increases with increasing surfactant concentration, even becoming bimodal at the higher concentrations.

The DT-1200 software contains a special presentation for justifying the transition from the log-normal to the bimodal distribution. It is based on the fitting error analysis. The software contains a searching procedure that looks for the log-normal and bimodal distributions that generate theoretical attenuation curves that fit the experimental data with the smallest errors. As a result,

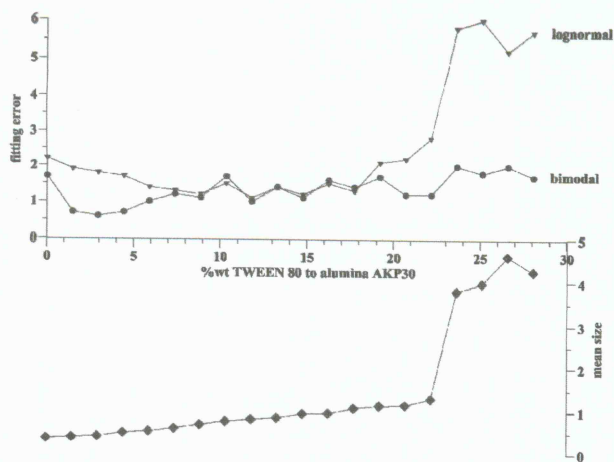


**Figure 10.** Fitting errors to the experimental attenuation curves for the alumina dispersion with different concentration of Tween 80 for a  $0.01 \text{ mol/dm}^3$  KCl solution.

we have two fitting errors—one corresponding to the log-normal distribution and the other corresponding to the bimodal. Figure 10 shows these fitting errors for the various attenuation curves from Figure 8. It is seen that the log-normal assumption is as good as the bimodal one up to 20% Tween 80. When the concentration of surfactant increases, the log-normal assumption fails. At this point, we can definitely claim that the particle size distribution becomes bimodal.

We have measured the attenuation spectra for all samples that are discussed above. This gives us the particle size information necessary to correct the  $\zeta$ -potential calculation properly. Practically all particle size distributions at ionic strengths above  $0.1 \text{ mmol/dm}^3$  are bimodal. It is important to reflect this feature of the particle size distribution. Otherwise, log-normal distributions would cause substantial error in the calculated  $\zeta$  potential.

LA050480D